



## Antibacterial and Wound Healing Effects of Chitosan-Silver Nanoparticle and Binahong (*Anredera cordifolia*) Gel Modified with Cinnamon Essential Oil

Nanda R.D. Lestari<sup>1</sup>, Sari E. Cahyaningrum<sup>1\*</sup>, Nuniek Herdyastuti<sup>1</sup>, Wahyu Setyarini<sup>2</sup>, Raditya Y. Arizandy<sup>1</sup>Department of Chemistry, Faculty of Mathematics and Natural Sciences, Universitas Negeri Surabaya. Jl. Ketintang, Gayungan, Surabaya 60231, East Java, Indonesia<sup>2</sup>Gastroenteritis Study Group, Institute of Tropical Disease, Universitas Airlangga. Jl. Dr. Ir. H. Soekarno, Mulyorejo, Surabaya 60115, East Java, Indonesia

### ARTICLE INFO

#### Article history:

Received 18 November 2023

Revised 12 December 2023

Accepted 18 December 2023

Published online 01 February 2024

**Copyright:** © 2024 Lestari *et al.* This is an open-access article distributed under the terms of the [Creative Commons Attribution License](https://creativecommons.org/licenses/by/4.0/), which permits unrestricted use, distribution, and reproduction in any medium, provided the original author and source are credited.

### ABSTRACT

Wound healing is a complex biological process that restores the skin structure to its original state following an injury. Improper wound treatment could lead to microbial infection. The extensive use of antibacterial drugs for the treatment of wound infections has encouraged the growth of multidrug-resistant bacteria, leading to the development of serious opportunistic infections. The use of gel formulations containing cinnamon essential oil (CEO) can prevent microbial infection and facilitates wound healing. This study is aimed at evaluating the antibacterial activity of chitosan (Chit)-silver nanoparticle (AgNp), and binahong leaf extract (BLE) gel modified with CEO against *Staphylococcus aureus*, and to investigate the gel's wound healing effect. The gel was formulated with CEO in different concentrations; 9, 7, 5, 3, 1, and 0% (without CEO). The physicochemical properties of the different formulations, including odour, colour, texture, homogeneity, pH, and spreadability, were assessed. The antibacterial and wound healing activities of the gel formulations were investigated in *Staphylococcus aureus* infected excision wound in Wistar rats. The gel modified with CEO has an average pH ranging from 4.53 to 5.16 and an average spreadability of 5.24 to 5.33 cm. The gel formulations at an optimum concentration of 7% CEO show significant antibacterial activity against *Staphylococcus aureus* with inhibition zone diameter of 19.5 mm. Histologically, gel formulations with CEO were found to exhibit significant wound healing effect. Overall, the results from the study suggest that gels formulated with CEO have the potential to be used as an alternative treatment for wound infection.

**Keywords:** Gel, Cinnamon essential oil, Antibacterial, Wound healing

### Introduction

Damage or loss of bodily tissue from external forces interfering with the body's defence mechanisms is referred to as a wound. Together with anatomical and physiological abnormalities, wound results in the disconnection of the skin epithelium.<sup>1</sup> Injuries need prompt medical attention since they can result in bleeding, microbial infection, tissue loss, and cell death. Wounds have been seen to be colonized by a wide range of microorganisms, including species found in normal skin microflora. The most prevalent species in these wounds is *Staphylococcus aureus*, which is found in 6.3 to 56.6% of cases.<sup>2</sup> The extensive use of antibacterial drugs to treat wound infections in hospitals has encouraged the growth of multidrug-resistant bacteria like *Staphylococcus aureus* and *Klebsiella sp.*, leading to the development of serious opportunistic infections that are challenging to treat.<sup>3</sup> For this reason, the quest for new antibacterial agents is therefore, essential. Generally, wound medicine preparations are in liquid or semi-solid forms, such as gel. Gels are a better healing alternative than liquid because they allow longer drug contact time than liquid, and could protect wounds from external influence.<sup>4</sup>

\*Corresponding author. E mail: [saricahyaningrum@unesa.ac.id](mailto:saricahyaningrum@unesa.ac.id)  
Tel: +62-812-3290-484

**Citation:** Lestari NRD, Cahyaningrum SE, Herdyastuti N, Setyarini W, Arizandy RY. Antibacterial and Wound Healing Effects of Chitosan-Silver Nanoparticle and Binahong (*Anredera cordifolia*) Gel Modified with Cinnamon Essential Oil. Trop J Nat Prod Res. 2024; 8(1):5936-5945. <http://www.doi.org/10.26538/tjnpr/v8i1.32>

Official Journal of Natural Product Research Group, Faculty of Pharmacy, University of Benin, Benin City, Nigeria.

This dosage form is easy to use and spreads quickly on the skin. Appropriate and effective gel preparations are expected to reduce and prevent wound infection.

Binahong leaf extract (BLE) and chitosan (Chit) are commonly used in wound healing applications. The wound-healing process in severe wounds can be hampered, giving rise to a biofilm layer of microbial colonies. Recent studies show that, due to its antibacterial properties, addition of silver nanoparticles (AgNp) could improve the antibacterial activity of gels.<sup>5,6</sup> Chitosan and nanosilver have emerged as promising materials in wound healing applications due to their synergistic antibacterial effects. In a study by Hajji *et al.*,<sup>7</sup> chitosan-PVA-silver nanoparticles (CSAgNPs) were prepared using a green method, with chitosan and PVA acting as stabilizing agents. The resulting CSAgNPs exhibited high antioxidant activity and low cytotoxicity, promoting significant wound healing in terms of contraction ratio and histological examination. Bagheri *et al.*,<sup>8</sup> developed chitosan/polyethylene oxide nanofibers incorporating antibacterial silver and zinc oxide nanoparticles, demonstrating high antioxidant and antibacterial activity against common wound pathogens. The nanofibers also showed biocompatibility, promoting fibroblast migration and proliferation. Cremar *et al.*,<sup>9</sup> produced chitosan-based composite fine fibers with silver nanoparticles and cinnamaldehyde, showing enhanced antibacterial activity against *Staphylococcus aureus* and providing effective three-dimensional substrates for cell adhesion and viability. Dahm,<sup>10</sup> discussed the role of silver and silver nanoparticles in wound infections, emphasizing their effectiveness against multidrug-resistant bacteria. Paladini and Pollini,<sup>11</sup> emphasized the urgent need for novel anti-biofilm strategies in wound management and the potential of silver nanoparticles in controlling infections and enhancing wound healing. However, excessive and careless use of these ingredients in treatment can cause resistance. Therefore, a modified gel has been developed using cinnamon essential oil (CEO).<sup>12</sup>

Cinnamon (*Cinnamomum verum*) is one of the medicinal herbs extensively found and used in Indonesia. It has a potential to be used in gel preparation for wound treatment due to the wound healing and antibacterial activities of its essential oil. CEO contains 68.73% cinnamaldehyde.<sup>13</sup> Cinnamaldehyde is a polyphenol derivative with antibacterial properties. Cinnamaldehyde has growth inhibitory effect against both gram-positive and gram-negative bacteria and also an inhibitor of biofilms formation.<sup>14</sup> CEO exhibits its antibacterial action by altering cell structure and membrane functionality, proteins and enzymes, or other essential processes involved in biosynthesis and energy generation.<sup>15,16</sup> CEO is also capable of altering the lipid profile of microbial cell membrane.<sup>17</sup> Furthermore, cinnamaldehyde in CEO accelerates wound healing by inducing angiogenesis in the wound area, speeding up the process of cell regeneration and proliferation.<sup>18</sup> The purpose of this study was to determine the antibacterial activity of Chit, AgNp, and BLE gel modified with CEO against *Staphylococcus aureus*, and to investigate the wound healing effect of the gel. The novelty of this research lies in the synergistic combination of Chit, AgNp, and BLE along with the modification using CEO to enhance the antibacterial properties and wound healing efficacy of the gel. The incorporation of CEO, which is known for its antibacterial activity and ability to accelerate wound healing, provides a novel approach to overcome microbial resistance. The study systematically evaluated the physicochemical properties including odour, colour, texture, homogeneity, pH, and spreadability of different gel formulations. The antibacterial tests against *Staphylococcus aureus* and *in vivo* activity tests in excision wound Wistar rats were conducted to validate the efficacy of the gel in preventing infections and promoting wound healing.

The methods adopted in this study encompass a comprehensive approach to developing and characterizing a novel gel formulation for wound healing. Phytochemical screening of BLE and CEO provides valuable insights into the chemical composition of the extracts, aiding in the understanding of their potential therapeutic effects. The synthesis of silver nanoparticle (AgNp) and its characterization contribute to the value of nanotechnology in modern research. The modification of gels with CEO and the subsequent characterization using Fourier Transform Infrared Spectroscopy (FTIR) demonstrate the integration of essential oils and their impact on the gel's functional groups. Stability tests, including organoleptic evaluation, homogeneity, spreadability, and pH measurement, were done to assess the applicability of the formulated gel. The antibacterial activity assessment against *Staphylococcus aureus* and the *in vivo* excision wound healing study in male Wistar rats demonstrated the translational potential and clinical relevance of the formulated gel. Histological examinations further enhance the understanding of the impact of the gel on cellular infiltration, collagen content, and angiogenesis.

## Materials and Methods

### Chemicals and biologicals

Aquadest, 96% ethanol pro analyses (Merck, Germany), 100% CEO (Naturalpedia, Indonesia), 99% chitosan (PT Acetyl Indo Megah, Indonesia), 100% glacial acetic acid (Sigma Aldrich, USA), Silver nitrate crystal (Merck, Germany), 99% sodium citrate dehydrate (Sigma Aldrich, USA), 99% propylene glycol (BuanaChem, Indonesia), xanthan gum (BuanaChem, Indonesia), Mueller Hinton (MH) agar (Oxoid, UK), Nutrient Broth (NB) (Oxoid, UK), and *Staphylococcus aureus* (Oxoid, UK).

### Equipment

The equipment used were; pH meter (smart sensor AS218, China), Fourier Transform Infrared (FTIR) spectrophotometer (PerkinElmer Spectrum Two, UK), Particle Size Analyzer (PSA) (Malvern Zeta Nanosizer, UK), Rotary evaporator (Buchi R-300, USA), Analytical balance (Ohaus Adventurer AR2140, UK), Magnetic stirrer with heater (DLAB MS-H280-Pro, USA), Incubator (Nesco DSI-500D, Taiwan), Microscope (Olympus BX53-P polarizing, Japan).

### Plants material

Fresh binahong (*Anredera cordifolia*) leaves Dep.Kes. RI No. SP 43712011999 were obtained from Yogyakarta (Indonesia) in May, 2023. The leaves were air dried and blended for further use.

### Extraction of binahong leaves

Dried binahong leaf powder was extracted by maceration in 96% ethanol at room temperature for 24 h. Three successive extractions were performed at sample to solvent ratios of 750 g: 2.250 mL for the first and second extractions, while the ratio for the third extraction was 750 g: 1.500 mL.<sup>5</sup> The combined extracts were filtered, and the filtrate was evaporated to dryness using a rotary evaporator at 65°C to obtain a dark green extract.

### Phytochemical screening of BLE and CEO

The procedure for Test Flavonoid, Alkaloid, Saponin, and Tannins described by Kumalasari and Andiarna.<sup>19</sup> The essential oil were prepared by the metode describe by Rivai *et al.*<sup>20</sup>

### Synthesis of Silver nanoparticle (AgNp)

Synthesis of silver nanoparticle was done by heating 50 mL of 1.0 mM AgNO<sub>3</sub> to boiling. To this solution was added 5 mL of 1% sodium citrate (Na<sub>3</sub>C<sub>6</sub>H<sub>5</sub>O<sub>7</sub>) dropwise. While heating, the mixture was stirred using a magnetic stirrer until it became pale yellow. The presence of pale yellow colour indicates formation of silver nanoparticle.<sup>21</sup>

### Characterization of AgNp with particle size analyzer (PSA)

The determination of particle size and distribution of silver nanoparticle was done by PSA instrument Malvern Zeta Nanosizer.

**Table 1:** Formulae used for the gel formulations of gel Chit, AgNp, BLE modified with CEO

Composition	Function	Formulas (% v/b)							
		F0	F1	F2	F3	F4	F5	F6	F7
Propylene glycol	Emulsifier	25	25	25	25	25	25	25	25
AgNp 7 ppm	Active ingredient	2.5	0	2.5	2.5	2.5	2.5	2.5	0
Chit 0.5%	Active ingredient	2.5	0	2.5	2.5	2.5	2.5	2.5	0
BLE	Active ingredient	0	0	5	5	5	5	5	5
CEO	Active ingredient	0	5	9	7	5	3	1	0
Xanthan gum	Gelling agent	2	2	2	2	2	2	2	2
Aquadest	Solvent	add	add	add	add	add	add	add	add
		100	100	100	100	100	100	100	100

Note: F0 (Chit-AgNp); F1 (CEO); F2 (Chit-AgNp-BLE-CEO 9%); F3 (Chit-AgNp-CEO 7%); F4 (Chit-AgNp-CEO 5%); F5 (Chit-AgNp-CEO 3%); F6 (Chit-AgNp-CEO 1%); F6 (BLE)

#### Preparation of CEO modified gels

The CEO modified gels were prepared by the method described by Aulia and Cahyaningrum<sup>5</sup> with slight modifications. Briefly, the gel formulations presented in Table 1 was initiated by heating 10 mL of water to 75°C. Then, propylene glycol and xanthan gum were added to a beaker and stirred quickly until dissolved and homogeneous. The temperature was then lowered to 65°C. At 65°C, 5% BLE<sup>5</sup> and CEO were subsequently added and stirred until homogeneous. Once homogeneous, the magnetic stirrer and heater were turned off, and then AgNp (7 ppm)<sup>22</sup> and Chit (0.5%)<sup>23,24</sup> solution were added to the beaker and stirred for 30 minutes until homogeneous. Finally, aquadest was added to a total weight of 20 g and stirred until homogeneous.

#### Characterization of gel with FTIR

The functional groups in the gel were analyzed using Fourier Transformed Infrared Spectroscopy (FTIR) at wave number range of 4.000-500 cm<sup>-1</sup>, using the Perkin Elmer Spectrum Two spectrophotometer.

#### Organoleptic properties and Stability testing of formulated gel

Organoleptic properties including; colour, aroma, and texture of the formulated gel were observed. The homogeneity test was carried out by smearing the gel on a glass plate and then observing whether there were no fine grains and whether the colour of the gel was evenly distributed.<sup>25</sup> The spreadability test was carried out by placing 0.5 g of the gel in the middle of a round glass scale, on top of which another transparent, round glass was placed and 150 g weight, allowed to stand for one minute, the diameter of the spread was recorded. Good gel spreadability is typically between 5 and 7 cm.<sup>26</sup> pH test and measurement on the gel preparations was done using a pH meter. The pH test was aimed to determine the pH of the formulation that is acceptable to the skin. Formulations are said to be good if they have a pH range between 4.5 and 6.5.<sup>25</sup>

#### Antibacterial activity screening

The antibacterial activity of the gel was tested using the disk diffusion method. The first step was to reheat the MH agar, which had previously been sterilized in the autoclave at 120°C for 15 min. Furthermore, rejuvenation of the pure culture of *Staphylococcus aureus* bacterial stock, which had previously been inoculated using NB media was done by taken one loop, then smeared on MH media and incubated at 37°C for 24 h. A bacterial suspension was prepared from the rejuvenated pure culture of the test bacteria and then inoculated into 5 mL of 0.9% sterile physiological NaCl solution. The bacterial density was calculated using the McFarland method. The turbidity of the test bacterial suspension was made uniform by using the McFarland standard 0.5 (bacterial density of 1.5 x 10<sup>8</sup> Colony Forming Units per mL (CFU/mL)).<sup>27</sup> Antibacterial activity test was carried out using paper disks dipped into the gel formulations F0 up to F7, positive control (ciprofloxacin), negative control (aquadest), and commercial binahong gel. The paper disks were placed in a petri dish containing MHA media inoculated with *Staphylococcus aureus*, then incubated at 37°C for 24 h. The clear inhibition zone was measured three times on each disk using a vernier calliper, and the values were averaged.<sup>5</sup> The clear inhibition zone is an indication of the sensitivity of bacteria to a test antibacterial substances, which is expressed by the diameter of the inhibition zone.<sup>28</sup>

#### Determination of wound healing activity

The procedure described by Ferro *et.al.*,<sup>29</sup> was used with slight modifications. Ethical clearance with reference No. 103-KEP-UB-2023 was obtained prior to the experiment. Briefly, male Wistar rats weighing 150 - 200 g were divided into six groups (A – F), with three rats in each group. Excision wounds were inflicted on anaesthetized rats by cutting away 300 mm<sup>2</sup> on each depilated rat and replaced. Each group was treated daily with the respective formulations for seven days. Each rat was provided with a separate cage, food, and water. Groups A, B, C, D, E, and F were treated with gel with formulation F0, F1, F3, F4, commercial binahong gel (positive control), and left untreated (negative control), respectively.

#### Histological examination of Wistar rat tissue (healed area)

The Wistar rat's tissue was treated with xylene and fixed in paraffin. Sections were cut from tissues of respective groups and stained with hematoxylin and eosin for microscopic examination. Furthermore, the slides were mounted with a mixture of distyrene, a plasticizer, and xylene (DPX) and observed for cellular infiltration, collagen content, and angiogenesis.<sup>30</sup> Qualitative observations were carried out using tissue and histological observations. Meanwhile, quantitative observations were made by counting fibroblasts, collagen density, and tissue angiogenesis on the tissue.

#### Statistical analysis

Data were presented as mean ± SEM. Data were subjected to One Way Analysis of Variance. Statistical significance difference was taken at P < 0.05. Comparison between means was done using Tukey Post Hoc test.

## Results and Discussion

#### Extraction Yield

The extraction procedure yielded a thick green extract of 63.33 g weight corresponding to a percentage yield of 8.44% (Table 2).

#### Phytochemical constituents of BLE and CEO

Phytochemical screening is a technique used to identify the secondary metabolites in a plant sample. Qualitative analysis of the phytochemicals was based on colour reaction. The results of the phytochemical screening of BLE and CEO are presented in Tables 3 and 4, respectively.

From the phytochemical screening results presented in Table 3, BLE contains flavonoids, saponins, alkaloids, and tannins, but essential oil was absent. This results agree with that of previous studies which showed that BLE contains flavonoids, tannins,<sup>31</sup> and saponins.<sup>5</sup> Essential oils were confirmed absent as no colour reaction was observed on addition of ethanol, hexane, acetone, and water extracts to potassium permanganate solution.

As shown in Table 4, CEO showed a positive test for alkaloids, flavonoids, tannins, and essential oils. This result corroborated that of the study by Panjaitan *et.al.*,<sup>32</sup> which showed that CEO contained flavonoids, tannins, and essential oil. Another study showed that CEO contained saponins and alkaloids.<sup>9</sup> The difference in the results of the phytochemical screening tests from several studies could be due to the extraction process which could have impacted the phytochemical constituents of CEO.<sup>15</sup>

#### Particle size of the silver nanoparticle

Characterizing particle size is paramount to determining the particle size of the silver nanoparticle (AgNp). Therefore, particle size analysis using the technique of light scattering on a sample particle with the PSA instrument was conducted in this study. The scattered light is inversely proportional to the size of the particle. Laser light disperses the particles and pass them through the beam laser. The results, which consist of scattering distribution and intensity, is analyzed by a computer and displayed as particle size distribution.<sup>28</sup> The result of the particle size analysis of the AgNp is displayed in Figure 1.

From Figure 1, there were mainly 31.16 nm sized particles in the studied nanoparticle solution. Small particles with a dimension of 1 to 100 nm are known as nanoparticles.<sup>33</sup> A wide range of industries, including technology, medical, and environmental cleanup, use nanoparticles. When employing nanoparticles in medicine, a maximum size of 200 nm is advised.<sup>34</sup> In this study, the particle size diameter of 31.16 nm falls within the nanoscale range, further confirming that the analyzed material indeed consists of nanoparticles. This also implies that the AgNp in this study are appropriately sized for various applications that utilize the unique properties exhibited by nanoparticles.

#### Fourier Transform Infrared (FTIR) spectroscopic data

The functional groups in the formulated gel were identified using FTIR. The working principle of FTIR is based on the absorption of infrared light by the vibrations of chemical bonds.<sup>28</sup> The FTIR spectrum is displayed in Figure 2.

The absorption peaks at wave numbers  $3,334.37\text{ cm}^{-1}$  and  $3,280.86\text{ cm}^{-1}$  in gel Chit-AgNp and gel CEO-BLE-Chit-AgNp, respectively, show typical absorption of the O-H stretch and N-H stretch vibrations that appear in the range of  $3,500$  to  $3,200\text{ cm}^{-1}$ .<sup>35</sup> The absorption peaks at  $585.70\text{ cm}^{-1}$  and  $587.05\text{ cm}^{-1}$  for gel CEO-BLE-Chit-AgNp and Chit-AgNp, respectively, is typical of C-O bending vibrations which appears in the range of  $500$  to  $1,500\text{ cm}^{-1}$ .<sup>36</sup> The peaks at  $1,636.31\text{ cm}^{-1}$  and  $1,639.32\text{ cm}^{-1}$  for gel Chit-AgNp and gel CEO-BLE-Chit-AgNp, respectively, are indicative of N-H bending which appears in the range of  $1,600$  to  $1,670\text{ cm}^{-1}$ .<sup>37</sup> The presence of these absorptions signify the presence of distinctive clusters of chitosan on the surfaces of gel AgNp and gel CEO-BLE-Chit-AgNp. Absorption at  $2,946.97\text{ cm}^{-1}$  indicates a stretching vibration C-H, suggesting that the aldehyde originated from the lipid group. Interaction between CEO and AgNp or Chit potentially affects the structure and characteristics of Chit-AgNp and CEO-BLE-Chit-AgNp.<sup>38</sup> The wavenumber of  $1281.27\text{ cm}^{-1}$  is associated with C-N stretching in aromatic amines which appear from  $1,342$  to  $1,266\text{ cm}^{-1}$ .<sup>39</sup> These peaks reveal Chit bonding with the aromatic groups of the CEO. The interaction between the CEO and components of chit is responsible for the observed FTIR spectral pattern.

#### Organoleptic Properties of the gel formulations

The findings from the sensory evaluation, as presented in Table 5, offer a full insight into the organoleptic attributes of the different gel formulations. The organoleptic attributes, comprising colour, aroma, and consistency, exert a significant influence on the overall desirability and sensory perception of the prepared gels. Firstly, with respect to colour, the formulations displayed a range of colour spanning from colourless to dark green. The observed colour change can be attributed to the different quantities of CEO and BLE contained in the gels. Most importantly, the presence of a dark green colour in formulations containing higher quantities of CEO and BLE indicates a more prominent impact of these natural extracts on the visual aspect of the gel.

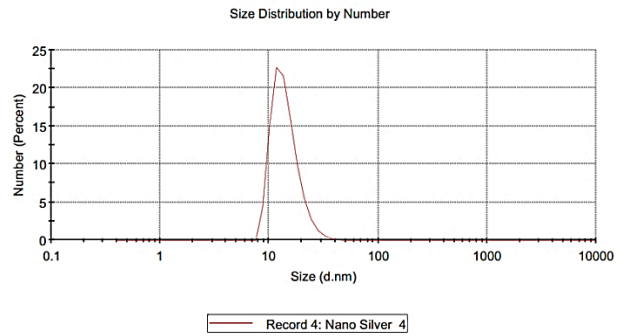


Figure 1: Particle size analysis result of AgNp

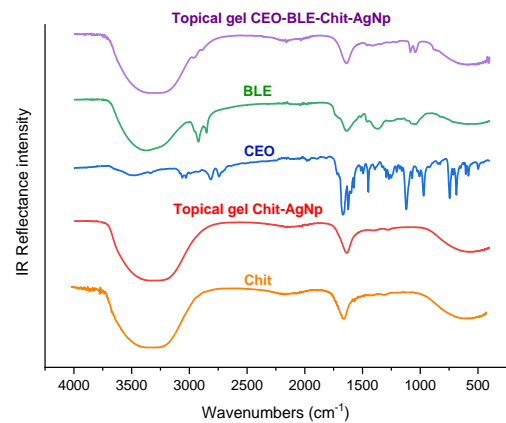


Figure 2: Infrared spectrum of Chit, BLE, CEO, Gel Chit-AgNp, and Gel CEO-BLE-Chit-AgNp.

Table 2: Extraction yield of BLE

	Weight of sample (g)	Weight of extract (g)	Yield (%)
Binahong leaves	750	63.33	8.44

Table 3: Phytochemical constituents of BLE

Phytochemical	Test	Observation	Inference
Alkaloid	Dragendroff	Orange precipitate	+
Flavonoid	Wilstater	Blackish-green	+
Saponin	Forth	Foamy	+
Tanin	FeCl <sub>3</sub> 1%	Green, brownish coloration	+
Essential oil	KMnO <sub>4</sub>	Purple	-

Note: (+) sign means present, (-) sign means absent

Table 4: Phytochemical constituents of CEO

Phytochemical	Test	Observation	Inference
Alkaloid	Dragendroff	No precipitate	-
Flavonoid	Wilstater	Yellow	+
Saponin	Forth	Not foamy	-
Tanin	FeCl <sub>3</sub> 1%	Blue, brownish coloration	+
Essential oil	KMnO <sub>4</sub>	Colorless	+

Note: (+) sign means present, (-) sign means absent.

With respect to the odour, it became apparent that the inclusion of cinnamon essential oil had a pronounced effect on the aromatic properties of the preparations. The olfactory perception was reported as negligible in the formulation without Chit-AgNp (F0), and mildly aromatic in the formulation containing solely BLE (F7). Nevertheless, as the concentrations of CEO increased, the odour changed from mildly strong to highly strong, thereby justifying the intense fragrance associated with cinnamon essential oil.

In relation to texture, all the formulations consistently displayed a semi-solid texture, as anticipated for gel formulations. The consistency in texture among the different formulations guarantees a consistent tactile encounter for individuals. The semi-solid nature of these gels plays a pivotal role in facilitating their application and ensuring the adherence to the intended purpose.

#### Homogeneity of the gel formulations

The findings from the homogeneity test, as shown in Table 6, offer insights into the consistency of the gel compositions over a four-week period. The attribute of homogeneity is of significant importance in pharmaceutical and cosmetic formulations due to its role in ensuring the constant distribution of active components. This characteristic is crucial as it helps minimize any potential complications arising from unequal dosing. Throughout the four-week testing period, all the formulations exhibited continuous homogeneity, irrespective of the proportion of CEO or the inclusion of BLE.

Homogeneity was maintained at each weekly interval for formulation F0 (Chit-AgNp) and F1 (CEO), which were used as the control groups. This finding suggests that the lack of CEO or BLE did not have a significant effect on the even distribution of components within the gel. In a similar manner, the formulations comprising different concentrations of CEO (F2 to F6) and those incorporating BLE (F7) demonstrated uniformity over a period of four weeks. This finding indicates that the inclusion of cinnamon essential oil at varying

concentrations or the concurrent presence of BLE extract did not adversely affect the general uniformity of the gel formulations. The observed uniformity exhibited by all formulations is a promising indication of the stability and reliability of the gel matrix. The presence of uniform distribution of components and the absence of phase separation are essential factors in maintaining the reproducibility of the gel's performance.

#### Spreadability of the gel formulations

The spreading test aim to see how simple it is to use or apply the gel. The results of the spreading power test are presented in Table 7. The active components could be absorbed faster due to the gel's wide skin contact and excellent spreading capabilities. The gels modified with CEO have an average spreading power of 5.24 to 5.33 cm. The outcomes satisfy the criteria for the spreading ability of the gel. This is because the gel size already falls within the necessary range of 5 and 7 cm.<sup>26</sup> Consequently, skin can be treated using this gel. It is important to note that increasing CEO affects the spreadability of the gel formulation.

#### pH of the gel formulations

The pH test aim to determine the acidity of the solution so that the gel pH could be adjusted accordingly. The pH of the gel formulations are shown in Table 8. The gel modified with CEO has an average pH ranging from 4.53 to 5.16, which correspond with the standard pH of the skin. When the pH of the gel is below 4.5, it becomes acidic and can irritate the skin. Meanwhile, when the pH of the gel is above 6.5, it becomes alkaline and can cause dryness and scaling of the skin.<sup>25</sup> The pH test results imply that addition of CEO can enhance the acidity of the gel. This is because essential oil in CEO is acidic. The present finding shows that increasing CEO decreases significantly the pH of the gel.

**Table 5:** Organoleptic properties of the gel formulations

Formulation	Colour	Odour	Texture
F0	Colourless	Odourless	Semi-solid
F1	Yellow	Cinnamon very pungent	Semi-solid
F2	Leaf green	Cinnamon very pungent	Semi-solid
F3	Leaf green	Cinnamon pungent	Semi-solid
F4	Green	Cinnamon pungent	Semi-solid
F5	Green	Cinnamon pungent	Semi-solid
F6	Dark green	Cinnamon slightly pungent	Semi-solid
F7	Dark green	Cinnamon non pungent	Semi-solid

Note: F0 (Chit-AgNp); F1 (CEO); F2 (Chit-AgNp-BLE-CEO 9%); F3 (Chit-AgNp-CEO 7%); F4 (Chit-AgNp-CEO 5%); F5 (Chit-AgNp-CEO 3%); F6 (Chit-AgNp-CEO 1%); F6 (BLE)

**Table 6:** Results of the homogeneity test of the different gel formulations

Formulation	Homogeneity			
	Week-1	Week-2	Week-3	Week-4
F0	Homogenized	Homogenized	Homogenized	Homogenized
F1	Homogenized	Homogenized	Homogenized	Homogenized
F2	Homogenized	Homogenized	Homogenized	Homogenized
F3	Homogenized	Homogenized	Homogenized	Homogenized
F4	Homogenized	Homogenized	Homogenized	Homogenized
F5	Homogenized	Homogenized	Homogenized	Homogenized
F6	Homogenized	Homogenized	Homogenized	Homogenized
F7	Homogenized	Homogenized	Homogenized	Homogenized

Note: F0 (Chit-AgNp); F1 (CEO); F2 (Chit-AgNp-BLE-CEO 9%); F3 (Chit-AgNp-CEO 7%); F4 (Chit-AgNp-CEO 5%); F5 (Chit-AgNp-CEO 3%); F6 (Chit-AgNp-CEO 1%); F6 (BLE)



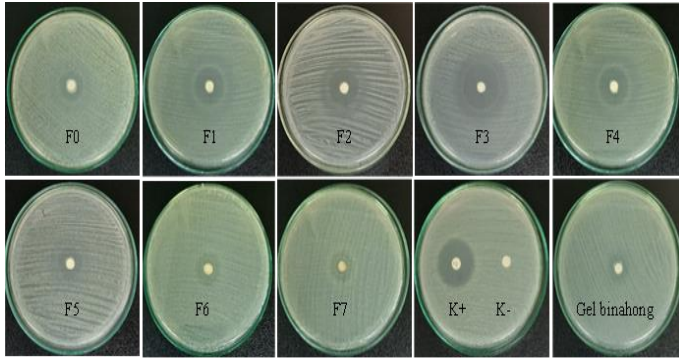


**Figure 3:** Antibacterial activity of the gel formulations against *Staphylococcus aureus*

#### Antibacterial Activity of the gel formulations

The antibacterial activity of the gel modified with CEO was tested against *Staphylococcus aureus* using the disc diffusion method. The results showed that the inclusion of CEO in the gel caused a higher bacterial growth inhibition than gel without CEO. The results of the antibacterial activity test were measured based on the inhibition zone diameter around the paper disk (Figure 3). The diameter of the inhibition zone was measured three times at different points and the values were averaged.<sup>40</sup>

Comparison of the antibacterial Activity of the different gel formulations as shown in Table 9, demonstrated that some samples (F0-F7) exhibited strong antibacterial activity, although not as strong as the positive control. The positive control exhibited the highest antibacterial activity among all tested samples and controls.

According to Aulia and Cahyaningrum,<sup>5</sup> BLE-Chit-AgNp gel with a concentration of 5% BLE is optimum as an antibacterial formulation against *Staphylococcus aureus*, with a diameter of inhibition zone of 13.04 mm. The diameter of inhibition zone against *Staphylococcus aureus* for BLE-Chit-AgNp gel was 4.2 mm. The differences in these inhibition zones may be due to the bacterial load, and/or the ingredients in the gel formulations. Therefore, modification of the gel with CEO could increase the antibacterial activity of binahong, chitosan and nanosilver. The largest zone of inhibition in the CEO-modified gel was seen at a CEO concentration of 7% with an inhibition diameter of 19.5 mm.

Cinnamaldehyde in CEO is an antibiofilm agent that destroys the layer regulated by microbes.<sup>41</sup> Biofilm can protect bacterial and fungal colonies from antibiotic compounds becoming resistant.<sup>42</sup> The dehydration process in the extracellular polymer matrix by cinnamaldehyde causes damage to the matrix and destroys the biofilm layer.<sup>29</sup> Once the microbial biofilm is destroyed, cinnamaldehyde will act as an antimicrobial. This result agree with previous research that cinnamaldehyde has been proven to have microbicidal activity against several types of bacteria, including; *S. aureus*, *S. epidermidis*, *S. pyogenes*, *P. aeruginosa*, and *E. coli*.<sup>17</sup> The formulation with the highest antibacterial activity as indicated by the largest zone of inhibition, was investigated for wound healing activity in male Wistar rats.

#### Wound Healing activity of the gel formulations

The results of the healing activity of excision wound in Wistar rats after seven days of treatment with the gel formulations are shown in Figure 4. The photomicrographs revealed the wound healing potential of CEO-modified gels (F1, F3 and F4) in excision wound of male Wistar rats after seven days of treatment.

**Table 7:** Results of the spreadability test of the different gel formulations

Formulation	Spreadability (cm)				Average
	Week-1	Week-2	Week-3	Week-4	
F0	5.30	5.29	5.33	5.32	5.31 ± 0.18
F1	5.28	5.29	5.33	5.31	5.30 ± 0.22
F2	5.29	5.28	5.29	5.30	5.29 ± 0.01
F3	5.33	5.30	5.34	5.37	5.33 ± 0.29
F4	5.31	5.29	5.30	5.31	5.30 ± 0.01
F5	5.26	5.25	5.27	5.28	5.26 ± 0.02
F6	5.24	5.23	5.23	5.25	5.24 ± 0.01
F7	5.27	5.29	5.26	5.25	5.27 ± 0.02

Note: F0 (Chit-AgNp); F1 (CEO); F2 (Chit-AgNp-BLE-CEO 9%); F3 (Chit-AgNp-CEO 7%); F4 (Chit-AgNp-CEO 5%); F5 (Chit-AgNp-CEO 3%); F6 (Chit-AgNp-CEO 1%); F6 (BLE)

**Table 8:** pH of the different gel formulations

Formulation	pH				Average
	Week-1	Week-2	Week-3	Week-4	
F0	4.53	4.51	4.58	4.50	4.53 ± 0.36
F1	4.74	4.73	4.73	4.76	4.74 ± 0.14
F2	4.81	4.82	4.78	4.83	4.81 ± 0.22
F3	4.91	4.94	4.90	4.93	4.92 ± 0.18
F4	4.96	4.95	4.97	4.96	4.96 ± 0.01
F5	4.99	4.99	5.10	4.95	5.01 ± 0.64
F6	5.00	4.99	5.12	5.05	5.01 ± 0.59
F7	5.20	5.22	5.13	5.11	5.16 ± 0.53

Note: F0 (Chit-AgNp); F1 (CEO); F2 (Chit-AgNp-BLE-CEO 9%); F3 (Chit-AgNp-CEO 7%); F4 (Chit-AgNp-CEO 5%); F5 (Chit-AgNp-CEO 3%); F6 (Chit-AgNp-CEO 1%); F6 (BLE)

**Table 9:** Inhibition zone Diameters of the gel formulations against *Staphylococcus aureus*

Formulation	Inhibition zone (mm)			Average
	1	2	3	
F0	6.8	6.7	6.9	6.8 ± 0.10
F1	18.4	19.2	20.3	19.3 ± 0.95
F2	19.6	16.4	21.4	19.1 ± 2.53
F3	19.5	20.5	18.4	19.5 ± 1.05
F4	18.9	18.6	20.3	19.3 ± 0.91
F5	20.8	17.8	18.5	19.0 ± 1.57
F6	16.6	18.6	13.8	16.3 ± 2.41
F7	3.8	4.3	4.5	4.2 ± 0.36
K+	20.0	20.4	19.6	20.0 ± 0.40
K-	0	0	0	0
Commercial Binahong gel	4.9	5.3	4.5	4.9 ± 0.40

Note: F0 (Chit-AgNp); F1 (CEO); F2 (Chit-AgNp-BLE-CEO 9%); F3 (Chit-AgNp-CEO 7%); F4 (Chit-AgNp-CEO 5%); F5 (Chit-AgNp-CEO 3%); F6 (Chit-AgNp-CEO 1%); F6 (BLE); K+ (ciprofloxacin); K- (aquadest)

**Table 10:** Infiltration of skin tissue in Wistar rats

Sample	Infiltration (cell)					Average
	1	2	3	4	5	
K+	0	0	0	0	0	11.80 ± 32.05
	59	60	58	0	0	
	0	0	0	0	0	
K-	138	55	53	73	94	71.33 ± 26.86
	55	60	51	40	49	
	106	65	101	64	63	
F0	30	37	35	44	45	44.86 ± 11.56
	45	61	43	34	35	
	52	51	52	73	36	
F1	52	47	33	34	47	43.33 ± 6.96
	45	43	52	51	49	
	38	49	36	34	40	
F3	0	0	0	0	0	10.86 ± 22.57
	0	0	0	0	0	
	0	0	49	58	56	
F4	30	35	24	46	42	28.93 ± 7.89
	29	28	21	24	19	
	36	28	22	29	21	

Note: K+ (commercial binahong gel); K- (without treatment); F0 (Chit-AgNp); F1 (CEO); F3 (Chit-AgNp-BLE-CEO 7%); F4 (Chit-AgNp-BLE-CEO 5%)

Different wound sizes were observed for treatment with gel with CEO, gel without CEO, commercial binahong gel, and untreated groups. Wounds generally heal from the third to the seventh day, and then stabilize and become organized around the fourteenth day. Angiogenesis starts on the third day, and fibroblasts begin producing new collagen on the fifth to seventh day. Cinnamaldehyde in CEO can promote angiogenesis via up-regulation of the phospho-inositide 3-kinase (PI3K) and the mitogen-activated protein kinase (MAPK) signalling at chronic wound sites. This signal is the recognition stage for cell proliferation and stimulates angiogenesis. Angiogenesis is an important stage in wound healing, which regenerates blood vessels and allow the supply of oxygen and other nutrients needed for cell repair, cell regeneration and blood vessel growth to the wound site. In addition,

cinnamaldehyde also increases the expression of Vascular Endothelial Growth Factor (VEGF) so that it can increase the number of endothelial cells, which help regenerate blood vessels.<sup>9</sup> The final stage is the matrix maturation or remodelling stage. Ursolic acid affects the activation and synthesis of transforming growth factor- $\beta$ 1 (TGF- $\beta$ 1) and modifies the TGF- $\beta$ 1 and TGF- $\beta$ 2 receptors on fibroblasts. This activation is an essential signal in the formation of collagen matrix in the matrix remodelling stage. Collagen will cover the epidermis layer of the skin so that the skin becomes normal again.

#### *Histological observation of Wistar Rat Tissue*

The wound healing process can be seen from the histological observation of the rat skin preparation (Figure 5). Tables 10 and 11

show cellular infiltration, collagen, and angiogenesis of the skin tissue on the seventh day following the excision process.

From the histology results, clouded inflammation was still found in groups treated with samples F1, F3, and F4 on the seventh day. Inflammation with the lowest inflammatory cells was found in the group treatment with F3, while in the control group, inflammatory cells were still found with infiltration cells more than that in F3. In theory, inflammatory cells in the wound-healing process tend to decrease over time. The number of inflammatory products found indicates the level of inflammation.<sup>30</sup> The faster the inflammatory products are reduced, the faster the healing process. Collagen production in the F3 treatment group was greater than in the control group. The wound healing observed on the seventh day of examination gradually increased until real wound closure was seen in the treatment and control groups. The new blood vessels found in the treatment group with the addition of CEO was better than that found in the treatment group without CEO. It can be seen that F1, F3, and F4 had a greater number of collagen and angiogenesis compared to the F0 group and the control group. In theory, collagen production appears to be higher for the healing process because collagen plays a role in repairing damaged or lost tissue. Fibroblasts lead to several phenotypic changes and become myofibroblasts, which help in wound retraction. Fibroblasts play a role in the formation of collagen to accelerate wound healing.<sup>31</sup> Meanwhile, angiogenesis occurs due to existing blood vessels giving off new blood vessel buds and shoots. Angiogenesis is pivotal in tissue repair to provide nutrients for regenerating tissue.<sup>9</sup> The more angiogenesis or new blood vessels are formed, the quicker the tissue repair, thereby accelerating the wound healing process.

## Conclusion

The integration of cinnamon essential oil (CEO) into gel formulations shown notable improvements in antibacterial efficacy and wound healing capabilities of the gels. The gels that were modified with CEO demonstrated significant reduction of *Staphylococcus aureus* growth. However, the antibacterial activity of these gels varied among different

formulations. Most importantly, the presence of cinnamaldehyde in CEO is associated with the strong antibiofilm activity by destroying the layers of microbial biofilms, hence augmenting the overall antimicrobial efficacy of the gels. The gels modified with CEO (F1, F3, and F4) exhibited enhanced wound closure, facilitated angiogenesis, mitigated inflammation, and augmented collagen synthesis in comparison to the control group. The histological data provided additional evidence to substantiate the enhanced tissue repair capabilities of the CEO-modified gels. In general, the present findings highlight the prospects of gels modified with CEO in enhancing skin health, addressing bacterial infections, and allowing effective wound healing. The findings from this study holds promise for driving future investigations that could significantly contribute to the field of wound healing.

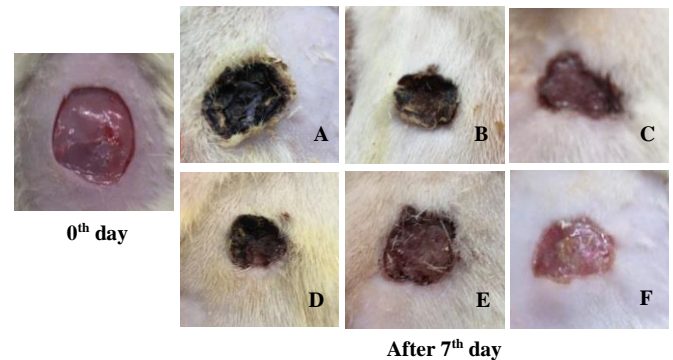


**Figure 4:** Excision wounds in Wistar rats at day 0 and after 7 days of treatment; (A) treated with F0; (B) treated with F1; (C) treated with F3, (D) treated with F4, (E) positive control; (F) negative control.

**Table 11:** Histological observation of the skin tissue

Sample	Collagen (%)					Average	Average groups	Angiogenesis (%)					Average	Average groups
	1	2	3	4	5			1	2	3	4	5		
K+	39.56	35.65	33.58	37.07	41.59	37.49		19	13	13	10	19	14.8	
	32.63	35.09	38.45	35.83	33.73	35.15	38.71 ± 4.65	16	11	11	16	17	14.2	16.0 ± 4.05
	41.44	41.22	40.78	44.27	49.83	43.51		25	21	16	16	17	19.0	
K-	34.56	33.02	37.17	35.95	34.76	35.09		9	12	9	8	8	9.2	
	29.93	31.91	27.93	28.03	30.71	29.70	31.88 ± 3.41	8	7	9	12	11	9.4	9.5 ± 3.62
	32.40	28.39	26.63	30.13	36.65	30.84		15	18	8	5	4	10.0	
F0	36.54	35.37	35.35	39.45	36.94	36.73		11	12	11	15	12	12.2	
	35.82	33.45	32.19	29.76	28.85	32.01	38.25 ± 6.44	13	10	10	8	12	10.6	11.3 ± 3.33
	48.26	47.04	47.00	41.07	46.64	46.00		11	6	14	6	19	11.2	
F1	38.73	33.61	45.18	45.74	36.72	39.97		15	12	11	11	10	11.8	
	38.36	37.61	36.26	37.63	39.61	46.91	40.62 ± 3.93	17	19	21	17	25	19.8	18.8 ± 6.34
	43.47	45.17	44.40	43.62	43.16	47.61		20	31	27	24	22	24.8	
F3	38.55	41.92	41.19	41.29	36.90	43.46		20	17	22	22	16	19.4	
	46.89	47.65	48.72	46.32	44.96	42.05	44.83 ± 3.93	14	17	15	14	23	16.6	18.8 ± 5.23
	46.66	49.05	49.35	45.20	47.80	41.67		19	13	17	19	34	20.4	
F4	41.53	42.26	44.62	45.84	43.02	40.00		23	11	17	19	17	17.4	
	41.02	45.05	40.97	41.42	41.80	37.90	42.39 ± 2.63	20	21	16	18	19	18.8	18.2 ± 3.86
	45.19	40.73	46.40	38.93	37.09	43.96		11	22	15	24	20	18.4	

Note: K+ (binahong gel on the market); K- (without treatment); F0 (Chit-AgNp); F1 (CEO); F3 (Chit-AgNp-BLE-CEO 7%); F4 (Chit-AgNp-BLE-CEO 5%)



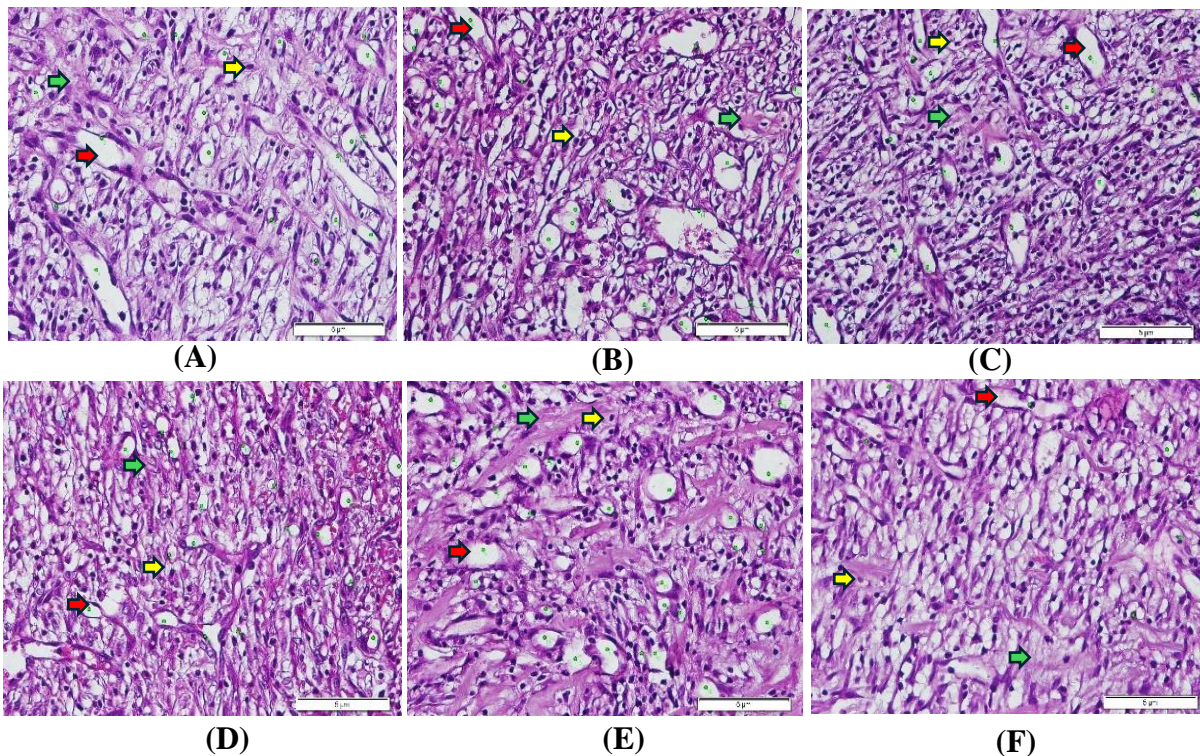


**Figure 5:** Photomicrographs of rat skin preparations (40x magnification). **Yellow arrows:** inflammatory cell infiltration; **Green arrows:** collagen density; **Red arrows:** angiogenesis. (A) treated with F0; (B) treated with F1; (C) treated with F3, (D) treated with F4, (E) positive control; (F) negative control.

### Conflict of Interest

The authors declare no conflict of interest.

### Authors' Declaration

The authors hereby declare that the work presented in this article is original and that any liability for claims relating to the content of this article will be borne by them.

### Acknowledgments

The authors are grateful to Direktorat Jenderal Pendidikan Tinggi Kementerian Pendidikan dan Kebudayaan Republik Indonesia (DRTPM), for supporting this research through Scheme Tesis Magister Research 2023 No. B/51252/UN38.III.1/LK.04.00/2023 on 20th June 2023.

### References

- Asri H, Adrianto AA, Fadhila N. The effectiveness of topical administration of noni fruit extract ointment with graded concentrations on the number of fibroblasts (research on male Wistar white rats made with incisions). *Medicoment J.* 2021; 1(1):7-12.
- Susanti PG and Cahyaningrum SE. Characterization and effectiveness test gel of Aloe vera combination chitosan as *Staphylococcus aureus* antibacterial. *UNESA J Chem.* 2022; 11(1):26-33.
- Mariani F and Galvan EM. *Staphylococcus aureus* in polymicrobial skin and soft tissue infections: Impact of interspecies interactions in disease outcome. *Antibiotics.* 2023; 12(7):1164.
- Theerdhala S and Harikrishnan N. Mupirocin loaded niosomal gel for topical wound healing applications. *Trop J Nat Prod Res.* 2023; 7(8):3676-3682.
- Aulia ID and Cahyaningrum SE. Characterization and antibacterial activity test of chitosan-silver nanoparticle gel and binahong leaf extract (*Anredera cordifolia* (Tenore) Steen) against *Staphylococcus aureus*. *J Pijar Mipa.* 2023; 18(4):650-658.
- Mirzajani F, Askari H, Hamzelou S, Schober Y, Römpf A, Ghassempour A, Spengler B. Proteomics study of silver nanoparticles toxicity on *Oryza sativa* L. *Ecotoxicol Environ Saf.* 2014; 108:335-339.
- Hajji S, Khedir SB, Hamza-Mnif I, Hamdi M, Jedidi I, Kallel R, Boufi S, Nasri, M. Biomedical potential of chitosan-silver nanoparticles with special reference to antioxidant, antibacterial, hemolytic and *in vivo* cutaneous wound healing effects. *Biochim Biophys Acta Gen Subj.* 2019; 1863(1):241-254.
- Bagheri M, Validi M, Gholipour A, Makvandi P, Sharifi E. Chitosan nanofiber biocomposites for potential wound healing applications: Antioxidant activity with synergic antibacterial effect. *Bioeng Transl Med.* 2021; e10254.
- Cremer L, Gutierrez J, Martinez J, A Materon L, Gilkerson R, Xu F, Lozano K. Development of antimicrobial chitosan based nanofiber dressings for wound healing applications. *Nanomed J.* 2018; 5(1):6-14.
- Dahm H. Chapter 9, Silver Nanoparticles in Wound Infections: Present Status and Future Prospects. In *Nanotech in Skin, Soft Tissue, and Bone Infec.* Springer. 2020.
- Paladini F and Pollini M. Antimicrobial Silver Nanoparticles for Wound Healing Application: Progress and Future Trends. *Materials.* 2019; 12(2540):1-16.
- Haryani Y, Kartika GF, Yuharmen Y, Putri EM., Alchalish DT, Melanie Y. Utilization of red ginger rhizome water extract (*Zingiber officinale* Linn. var. *rubrum*) for simple biosynthesis of silver nanoparticles. *Chimica et Natura Acta.* 2016; 4(3):151-155.
- Inayati I, Arifin NH, Febriansah R, Indarto D, Suryawati B, Hartono H. Trans-cinnamaldehyde inhibitory activity against

- mrkA, treC, and luxS genes in biofilm-forming *Klebsiella pneumoniae*: An *in silico* study. Trop J. Nat Prod Res. 2023; 7(10):4249-4255.
14. Yuan X, Han L, Fu P, Zeng H, Lv C, Chang W, Runyon RS, Ishii M, Han L, Liu K, Fan T, Zhang W, Liu R. Cinnamaldehyde accelerates wound healing by promoting angiogenesis via up-regulation of PI3K and MAPK signaling pathways. Lab Invest. 2018; 98(6):783-798.
  15. Kim Y, Kim S, Cho KH, Lee JH, Lee J. Antibiofilm activities of cinnamaldehyde analogs against uropathogenic *Escherichia coli* and *Staphylococcus aureus*. Int J Mol Sci. 2022; 23(13):7225.
  16. Mousavi F, Bojko B, Bessonneau V, Pawliszyn J. Cinnamaldehyde characterization as an antibacterial agent toward *E. coli* metabolic profile using 96-blade solid-phase microextraction coupled to liquid chromatography–mass spectrometry. J Proteome Res. 2016; 15(3):963-975.
  17. Firmino DF, Cavalcante TTA, Gomes GA, Firmino NCS, Rosa LD, de Carvalho MG, Catunda FEA Jr. Antibacterial and antibiofilm activities of *Cinnamomum sp.* essential oil and cinnamaldehyde: Antimicrobial activities. Sci World J. 2018; 2018:7405736.
  18. Pang D, Huang Z, Li Q, Wang E, Liao S, Li E, Zou Y, Wang W. Antibacterial mechanism of cinnamaldehyde: Modulation of biosynthesis of phosphatidylethanolamine and phosphatidylglycerol in *Staphylococcus aureus* and *Escherichia coli*. J Agric Food Chem. 2021; 69(45):13628-13636.
  19. Kumalasari ML and Andiarna F. Phytochemical test of ethanol extract of basil leaves (*Ocimum basilicum L.*). Indones J. Heal Sc. 2020; 4(1):39-44.
  20. Rivai H, Misfadhila S, Sari LK. Qualitative and Quantitative Analysis of Chemical Contents of Hexane, Acetone, Ethanol and Water Extracts from Turmeric Rhizomes (*Curcuma domestica* Val). J Sains Farmasi & Klinis. 2019; March:1-16.
  21. Ariyanta HA. Silver nanoparticles preparation by reduction method and its application as antibacterial for cause of wound infection. J MKMI. 2016; 10(1):36-42.
  22. Ydollahi M, Ahari H, Anvar AA. Antibacterial activity of silver-nanoparticles against *Staphylococcus aureus*. Afr J Microbiol Res. 2016; 10(23):850-855.
  23. Simanjuntak RCM, Rlyoly W, Fretes FD, Gintu AR. Biofilm chitosan as modern dressing for ulcers. JKPK. 2021; 6(3):335-342.
  24. Magani AK, Tallei TE, Kolondam BJ. Antibacterial test of chitosan nanoparticles against *Staphylococcus aureus* and *Escherichia coli*. J Bios Logos. 2020; 10(1):7-12.
  25. Emelda E, Husein S, Saputri D, Yolanda. Formulation and testing of physical properties of single gel preparations and combinations of ethanolic extracts of red betel leaves (*Piper crocatum*) and cinnamon oil. Inpharmmed J. 2020; 4(2):43-53.
  26. Alsarra IA. Chitosan topical gel formulation in the management of burn wounds. Int J Biol Macromol. 2009; 45(1):16-21.
  27. Nurhayati LS, Yahdiyani N, Hidayatulloh A. Comparison of the antibacterial activity of yogurt starter with disk diffusion agar and well diffusion agar methods. J Teknologi Hasil Peternakan. 2020; 1(2):41-46.
  28. Lestari NR and Cahyaningrum SE. Synthesis and characterization of hydroxyapatite - nanopartikel as anti bacteria that cause dental caries. Indo J Chem Sci. 2022; 11(1):33-40.
  29. Ferro TA, Araújo JM, Dos Santos Pinto BL, Dos Santos JS, Souza EB, da Silva BL, Colares VL, Novais TM, Filho CM, Struve C, Calixto JB, Monteiro-Neto V, da Silva LC, Fernandes ES. Cinnamaldehyde inhibits *Staphylococcus aureus* virulence factors and protects against infection in a *Galleria mellonella* model. Front Microbiol. 2016; 21(7):2052
  30. Quazi A, Patwekar M, Patwekar F, Mezni A, Ahmad I, Islam F. Evaluation of wound healing activity (excision wound model) of ointment prepared from infusion extract of polyherbal tea bag formulation in diabetes-induced rats. Evid Based Complement Alternat Med. 2022; 2022:1372199.
  31. Kintoko K, Karimatulhaji H, Elfasyari TY, Ihsan EA, Putra TA, Hariadi P, Ariani C, Nurkhasanah, N. Effect of diabetes condition on topical treatment of binahong leaf fraction in wound healing process. Trad Med J. 2017; 22(2):103-110.
  32. Panjaitan CC, Widyarman AS, Amtha R, Astoeti TE. Antimicrobial and antibiofilm activity of cinnamon (*Cinnamomum burmanii*) extract on periodontal pathogens-an *in vitro* study. Eur J Dent. 2022; 16(4):938-946.
  33. Nugroho B and Cahyaningrum SE. Synthesis and characterization of hydroxyapatite-nanosilver-clove oil (*Eugenia caryophyllus*) as antibacterial in toothpaste preparations against *Streptococcus mutans* bacteria. J. Pijar Mipa. 2023; 18(4):659-665.
  34. Chenthamara D, Subramaniam S, Ramakrishnan SG, Krishnaswamy S, Essa MM, Lin F, Qoroffleh MW. Therapeutic efficacy of nanoparticles and routes of administration. Biomater Res. 2019; 23(20).
  35. Abdussalam MW, Mohamed L, Abraheem MS, Mansour MMA., Sherif AM. Biofabrication of silver nanoparticles using *teucrium apollinis* extract: characterization, stability, and their antibacterial activities. Chem. 2023; 5(1):54-64.
  36. Sikorski D, Bauer M, Frączyk J, Draczyński Z. Antibacterial and antifungal properties of modified chitosan nonwovens. Polym. 2022; 14(9):1-17.
  37. Ramalingam B, Khan MR, Mondal B, Mandal AB, Das SK. Facile synthesis of silver nanoparticles decorated magnetic-chitosan microsphere for efficient removal of dyes and microbial contaminants. ACS Sustainable Chem Eng. 2015; 3(9):2291-2302.
  38. Li Y and Kong DW. Analysis and evaluation of essential oil components of cinnamon barks using GC-MS and FTIR spectroscopy. Ind Crop Prod. 2013; 41:269-278.
  39. Behrooz AB, Fereshteh F, Fahimeh LA, Moones V, Farideh TY. Chemical composition and antioxidant, antimicrobial, and antiproliferative activities of *Cinnamomum zeylanicum* bark essential oil. Evid-Based Complement Alternat Med. 2020; 2020:1-8.
  40. Muhaimin FI, Cahyaningrum SE, Lawarti RA, Maharani DK. Characterization and antibacterial activity assessment of hydroxyapatite-betel leaf extract formulation against *Streptococcus mutans in vitro* and *in vivo*. Indo J Chem. 2023; 23(2):358-369.
  41. Utamia DT, Hertianib T, Pratiwib SU, Haniastuti T, Randy A, Priyanto JA, et al. Correlation analyses of the oral biofilm growth inhibition towards hydrophobicity reduction of oral pathogenic bacteria. Trop J. Nat Prod Res. 2023; 7(10):4141-4145.
  42. Herdyastuti N, Fauziah Widodo R, Prabowo YY, Apriliana IA, Cahyaningrum SE. Diversity of chitinolytic bacteria from shrimp farms and their antifungal activity. J Nat Sci Bio Med. 2021; 12(3):317-324.